J Electr Eng Technol.2018; 13(3): 1131-1137
http://doi.org/10.5370/JEET.2018.13.3.1131

ISSN(Print) 1975-0102
ISSN(Online) 2093-7423

A Novel Control Algorithm of a Three-phase Four-wire PV Inverter with Imbalance Load Compensation Function

Dinh-Vuong Le*, Chang-Soon Kim*, Byeong-Soo Go*, Minwon Park† and In-Keun Yu*

Abstract – In this paper, the authors suggest a new control algorithm for a three-phase four-wire photovoltaic (PV) inverter with imbalance load compensation function using conventional proportional-integral (PI) controllers. The maximum power of PV panel is calculated by the MPPT control loop. The reference varying signals of current controllers are transformed to two different rotating frames where they become constant signals. Then simple PI controllers are applied to achieve zero steady-state error of the controllers. The proposed control algorithm are modeled and simulated with imbalance load configuration to verify its performance. The simulation results show that the maximum PV power is transferred to the grid and the imbalance power is compensated successfully by the proposed control algorithm. The inverter has a fast response (~4 cycles) during the transient period. The proposed control algorithm can be effectively utilized to the three-phase four-wire inverter with imbalance load compensation function.

Keywords: Imbalance load, Control algorithm, PI controller, Three-phase four-wire inverter.

1. Introduction

In recent years, along with the use of the renewable energy sources such as photovoltaic (PV), wind, or biomass, the structure of the power system has been changed and become more complex. A new concept of the power system is introduced and called widely as microgrid. In this concept, small-scale distributed generators which generate electrical power from various primary energy sources such as wind, diesel, biomass, and PV are connected throughout the power network by both three-phase and single-phase connection. The power network becomes more flexible, controllable, and environment-friendly but also faces many new challenges due to its complexity [1-3]. As a consequence, the imbalance power of three-phase power network becomes one of the challenges of the microgrid.

The small neutral current caused by slightly imbalance phase currents is not a problem for the microgrid system and does not affect the distributed generator. However, when imbalance load increases, the neutral current becomes higher. A high neutral current can cause system failures or damage the generator by including pulsating torque [3-5]. Particularly, the imbalance power causes increasing heat loss on the magnetic core of transformer which is a component of a grid-connected microgrid due to imbalance magnetic field. Consequently, the efficiency, reliability, and power quality of the microgrid are reduced.

Besides the growth of renewable energy and semi-conductor devices, the multi-function inverter has being developed rapidly to take advantages of renewable energy and increase the power quality of the grid. A three-phase four-wire PV inverter is not only able to transfer maximum power from PV panels to a grid network but also compensate the imbalance power load. The most difficulty in the three-phase four-wire PV inverter with imbalance load compensation function is controller design which has varying reference signals [3, 4-8].

Deadbeat, fuzzy, hysteresis or hybrid resonant controllers which are used to control the varying reference signal have been used for active power filter. Therefore, these controllers can be applied to the PV inverter with imbalance compensating function. However, the common drawbacks of these controllers are sensitive to noise, huge computation work, and high implementation cost. Furthermore, in industrial or commercial PV inverter, the Proportional-Integral (PI) controller is preferably used because of its stability to noise, simplicity and low implementation cost [5, 7-12].

In this paper, the authors suggest a new control algorithm for a three-phase four-wire PV inverter with imbalance load compensation function using conventional PI controllers in two different rotating reference frames. A 40 kW building load composed of three single phase loads and a three-phase four-wire PV inverter are simulated to verify the performance of the proposed control algorithm. The control algorithm includes two control loops. A Phase Lock-loop (PLL) is used to synchronize phase angle and frequency of the PV inverter to the grid. The current controller is used to control power flow to the grid and compensate the imbalance load. The reference signal of the current control loop is transformed to 60 Hz rotating frame

† Corresponding Author: Dept. of Electrical Engineering, Changwon National University, Korea. (duku@changwon.ac.kr)
* Dept. of Electrical Engineering, Changwon National University, Korea. ({vuongld.elec, ee.cskim, iopewq1}@gmail.com, yuik@changwon.ac.kr)
Received: September 17, 2017; Accepted: February 7, 2018

then decomposed by the low-pass filter into two parts, a constant and a varying reference signals. Then, the varying reference signal is transformed to another rotating reference frame (120 Hz) where it becomes constant. Then PI controllers are applied at the two rotating reference frames to transfer maximum power from PV panels into the grid and compensate imbalance load while ensure zero steady-state error. The coefficients of the PI controllers are easily achieved after a few simple calculation steps. Consequently the proposed control algorithm improves the overall performance of the three-phase four-wire PV inverter system.

2. Controller Design

2.1 Modelling of a three-phase four-wire

The circuit diagram of a three-phase four-wire PV inverter is presented in Fig. 1. There are six IGBTs in 3 legs and the fourth leg is made by a coupling capacitor. The inverter has two functions which are transferring the maximum power from PV to the grid and compensating the imbalance power between three phases.

Neglecting the capacitor C_f, the PV inverter can be defined as in (1).

$$\bar{v}_p(t) = R\bar{i}(t) + L\frac{d}{dt}\bar{i}(t) + \bar{v}_g(t) \quad (1)$$

where $R = R_{L1} + R_{L2}$, $L = L_1 + L_2$. L_1, L_2, R_{L1}, R_{L2} are the inductance and resistance of inductor L_1, L_2, respectively. $\bar{v}_p(t)$ is inverter-side voltage space vector, $\bar{v}_g(t)$ is grid voltage space vector, and $\bar{i}(t)$ is the inverter current space vector.

By using the dq-transformation, all time-varying variables in the stationary frame of the inverter system become constant (DC) variables in a rotating reference frame (60Hz). The PV inverter, therefore, has dynamic response characteristic the same as a DC-DC converter and is much easier in analysis and control.

The dq-transformation between the stationary and rotating frame is defined, as (2).

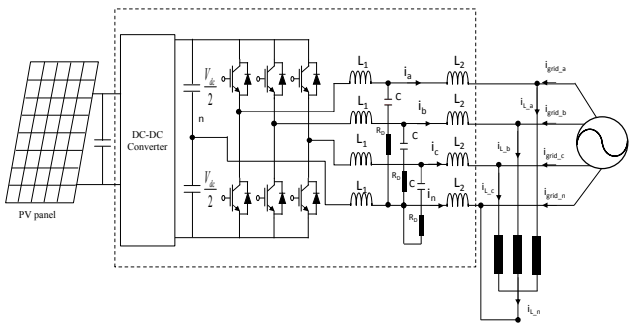

Fig. 1. Circuit diagram of a three-phase four-wire PV inverter

$$T_1 = \frac{2}{3}\begin{bmatrix} \cos(\omega t) & \cos(\omega t + 2\pi/3) & \cos(\omega t + 4\pi/3) \\ \sin(\omega t) & \sin(\omega t + 2\pi/3) & \sin(\omega t + 4\pi/3) \\ 0.5 & 0.5 & 0.5 \end{bmatrix} \quad (2)$$

where ω is the angular velocity of the rotating frame as well as the fundamental angular velocity of the grid.

In the rotating frame, the inverter model is illustrated by the Kirchhoff's laws in d- and q-axis written as (3), the current and voltage in 0-axis in this function is zero and neglected.

$$\begin{cases} v_d(t) = Ri_d(t) + L\frac{d}{dt}i_d(t) + v_{g-d}(t) - \omega L i_q(t) \\ v_q(t) = Ri_q(t) + L\frac{d}{dt}i_q(t) + v_{g-q}(t) + \omega L i_d(t) \end{cases} \quad (3)$$

So the dq currents are controlled by adjusting the voltage difference between the PV inverter ($v_{d,q}(t)$) and the grid ($v_{g\text{-}d,q}(t)$). Two general PI controllers are applied to generate the desired voltages.

2.2 Proposed control algorithm

The overall diagram of the proposed control algorithm is presented in Fig. 2. The first function is performed by a PI controller as the same as a conventional three-phase PV inverter which controls independently active and reactive power into the power grid. This function is implemented in a 60 Hz rotating reference frame.

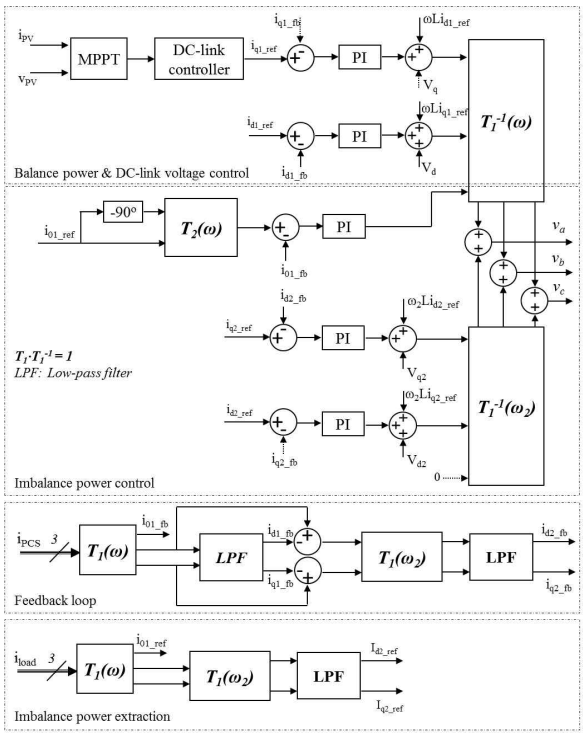

Fig. 2. Control algorithm of the inverter

The second function of the inverter is imbalance load compensation. The compensating power is computed by an imbalance power extraction method which includes the dq-transformation and a low-pass filter, as depicted in Fig. 2. The single-load powers of are measured by current sensors and then are transformed into the 60Hz- rotating frame by the same transformation T_1. In the d-, and q-axis, the signals varying due to the imbalance load current are composed of two different frequency signals ($0\cdot\omega$ *and* $2\cdot\omega$). The $0\cdot\omega$- (DC) signal represents the balance power part of the load. The $2\cdot\omega$-frequency signals in d-, q-axis and the ω-frequency signal in 0-axis represent the imbalance power part of the load. The ω_2-frequency signals ($\omega_2 = 2\cdot\omega$) in d-, q-axis (i_{d2_ref}, i_{q2_ref}) and the ω-frequency signal at 0-axis are written as in (4).

$$\begin{aligned}
\frac{3}{3} i_{d2_ref} &= \mathrm{I_a}\cos(\omega_2 t) + \mathrm{I}_b \cos\left(\omega_2 t + \frac{2\pi}{3}\right) + \mathrm{I}_c \cos\left(\omega_2 t + \frac{4\pi}{3}\right) \\
\frac{3}{2} i_{q2_ref} &= \mathrm{I_a}\sin(\omega_2 t) + \mathrm{I}_b \sin\left(\omega_2 t + \frac{2\pi}{3}\right) + \mathrm{I}_c \sin\left(\omega_2 t + \frac{4\pi}{3}\right) \\
\frac{3}{2} i_{02_ref} &= \mathrm{I_a}\sin(\omega t) + \mathrm{I}_b \sin\left(\omega t + \frac{2\pi}{3}\right) + \mathrm{I}_c \sin\left(\omega t + \frac{4\pi}{3}\right) \\
&\rightarrow \begin{cases} i_{d2_ref} = \mathrm{I}_{d2}\cos(\omega_2 t + \varphi_d) \\ i_{q2_ref} = \mathrm{I}_{q2}\sin(\omega_2 t + \varphi_q) \\ i_{02_ref} = \mathrm{I}_{02}\sin(\omega t + \varphi_0) \end{cases} \qquad (4)
\end{aligned}$$

where I_a, I_b, and I_c, are the magnitude of load current in phase A, B, and C, respectively.

The i_{d2_ref}, i_{q2_ref} signals become the reference signals for the inverter to compensate the imbalance power of the load. Since these signals have 90-degree phase angle difference, the $\alpha\beta$-$dq0$ transformation is used to transform these sinusoidal signals to constant signals at a rotating reference frame ($2\cdot\omega$~120 Hz). The $\alpha\beta$-$dq0$ transformation is defined as (5).

$$T_2 = \begin{bmatrix} \cos(\omega_2 t) & \sin(\omega_2 t) \\ -\sin(\omega_2 t) & \cos(\omega_2 t) \end{bmatrix} \qquad (5)$$

In the 120-Hz rotating frame, a part of compensated power, now, is represented by the DC signals which are easily regulated by simple PI controllers.

Particularly, in the 0-axis, the i_{0r} signal is a 60 Hz sinusoidal signal which is insufficient for the PI controller. An orthogonal signal (90-degree phase angle difference) of the i_{0r} signal is created then using the $\alpha\beta$-$dq0$ transformation, as in (5) with $2\pi 60$ *rad/s* of the angular velocity, to transform these signals to the 60Hz-rotating frame where they become DC signals. So the imbalance load power, now, is comprehensively represented by the DC signals at d-, q-axis in 120 Hz rotating frame and 0-axis in 60 Hz rotating frame which are efficiently controlled by PI controllers.

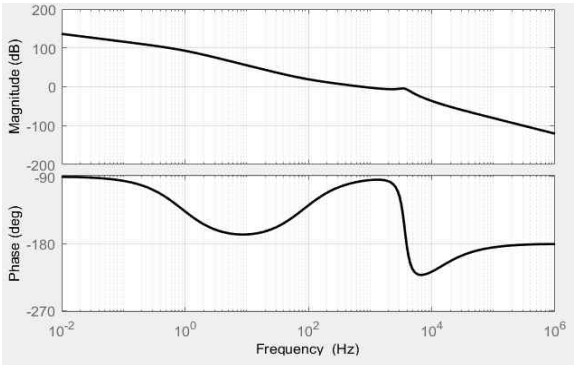

Fig. 3. Bode plot of the inverter open loop

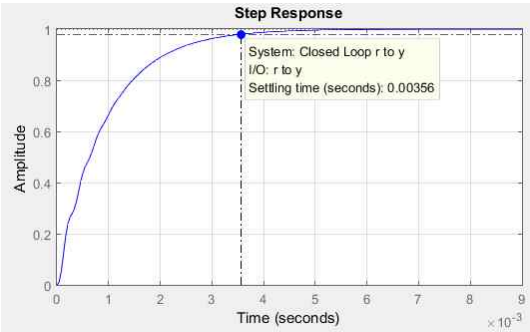

Fig. 4. The step response of the inverter closed loop

The inverter is controlled in the two different rotating reference frames. However, since the dynamic characteristics of the inverter are the same in both two reference frames, the model of the inverter in the two reference frames are the same too. Therefore, both controllers in the two reference frames are the same and designed as one.

The dc-link voltage is maintained by a simple PI controller which generally has small coefficients (smaller than 1). The maximum power of PV panel is calculated by the MPPT control loop which is controlled by the inverter's controller in the 60 Hz-rotating reference frame (dq_1). The measured signals from load are firstly transformed from stationary frame to the dq1 frame and filtered by the high-pass filter to obtain the varying signals which represent the imbalance power load. Then the signals are once again converted to the 120 Hz rotating frame (dq_2) to become constant signals which are the reference signals of the PI controller. In particular, the 0-axis component and its orthogonal signal (90-degree difference) is created and then transformed to the dq1 frame where it becomes DC signal. The feedback signals of output inverter are obtained by the same process. The controllers' output signals are inversely transformed to the stationary frame and then added together to obtain the signal which is used for pulse-width-modulation block. The inverter system has the specifications as represented Table 1. The coefficients of the PI controllers are calculated easily by the zero/pole placement method and the bandwidth criterion (570 Hz), as in (6). The stability of the inverter is verified by the phase

Table 1. The specifications of the PV inverter

Parameters	Values
Inverter-side inductor L_1	3.0 mH – 0.01 Ω
Grid-side inductor L_2	1.5 mH – 0.01 Ω
Filter capacitor C_f	2.2 µF
Damping resistor R_D	7 Ω
DC-link voltage	700 V
Switching frequency	10 kHz

margin of the system that is 85° at 570 Hz (3.6e3 rad/s) of cut-off frequency, as in Fig. 3. The step response of the inverter system is approximately 3.5 ms as illustrated in Fig. 4.

$$\begin{cases} \dfrac{k_p}{k_i} = \dfrac{L_1 + L_2}{R_{L1} + R_{L2}} \\ \left| \dfrac{k_p s + k_i}{s} G(s) \right|_{570Hz} = 1 \end{cases} \quad (6)$$

$$G(s) = \frac{z_C(s)\left(z_{L1}(s) + z_{L2}(s)\right) + z_{L1}(s) z_{L2}(s)}{z_C(s)}$$

where k_i, k_p are the coefficients of the PI controller. $G(s)$ is the transfer function of the inverter filter. z_C, z_{L1}, z_{L2} are the impedances of the inductor L_1, L_2, and the capacitor C_f including R_D in Laplace domain, respectively.

Contrary to the dead-beat, hysteresis, or resonant controllers which generally require an accurate model of the inverter and huge calculation to obtain and implement these controllers, the proposed control algorithm need a simple inverter model and conventional PI controllers. The inverter model and coefficients of the PI controllers are easily achieved after a few simple calculation steps. Furthermore, the PI controllers ensure zero steady-state and consequently improve the overall performance of the inverter system.

3. Simulation and Results

The model of a three-phase four-wire PV inverter with a PV panel as shown in Fig. 1 is simulated by using PSIM. The parameters of the PV inverter are the same as Table 1. Three single-phase loads that have total 40 kW of power is used to simulate imbalance load condition. The PV power is harvested by a DC-DC converter which has the MPPT control loop. Then the inverter part transfers power to the grid. To confirm the performance of the controller, the inverter is simulated in three case studies:

- Imbalance power smaller than the maximum PV power
- Imbalance power is higher than the maximum PV power
- Transient conditions

The standard deviation (s) which is used to quantify the amount of variation or dispersion of a set data values in statistics is applied to evaluate the imbalance power. The standard deviation of three-phase power is calculated as (7).

$$s = \sqrt{\frac{1}{3}\left[\left(p_A - \bar{p}\right)^2 + \left(p_B - \bar{p}\right)^2 + \left(p_C - \bar{p}\right)^2\right]} \quad (7)$$

where p_A, p_B, p_C are the power of phase A, B, and C, respectively. $\bar{p}$ is the average value of p_A, p_B, and p_C.

3.1 Case study 1: Imbalance power smaller than the maximum PV power

In this simulation, the load powers are 20 kW, 10 kW and 10 kW, respectively of phase A, B, and C. The standard

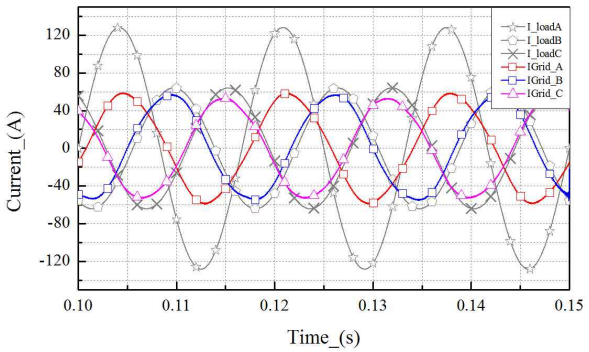

(a) The grid and load currents in steady-state

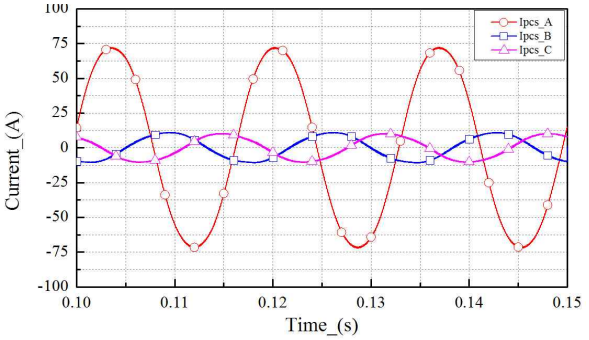

(b) The inverter output current waveforms

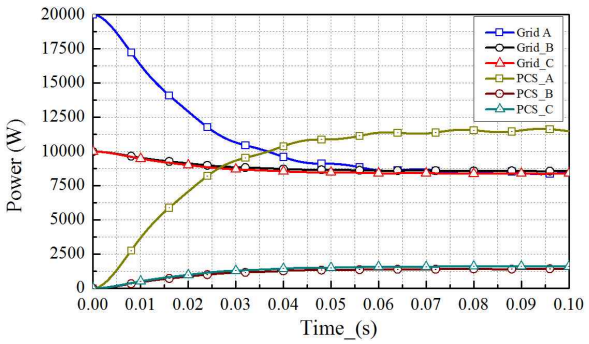

(c) Power of load, grid, and inverter output

Fig. 5. Imbalance load compensation with PV power

deviation of the load power is 4.714. The maximum PV output power is approximately 15 kW. The simulation results are presented in Fig. 5. If the inverter transfers 10 kW power to the grid by phase A, then the power is balance from the grid at 10 kW of each phase. But the PV power still remains approximately 5 kW, so the remained power is continuously transferred to the grid by all three phases (1/3 of remained power on each phase). We can see the grid power is balance around 8.5 kW (8.612 kW on phase A and B, 8.45 kW on phase C) which is lower than average load power (13.3 kW). It means that the imbalance load is totally covered by the PV power. The magnitudes of the inverter output currents are imbalanced but their phases are balanced as in Fig. 5(b). It means that the inverter does not receive any power from the grid during the operation. The inverter output powers on three phases are positive value as in Fig. 5(c). By using the inverter for compensating imbalance load power, the standard deviation of the grid power is 0.1824 which is much smaller than one of load power (4.714).

3.2 Case study 2: Imbalance power is higher than the maximum PV power

The load powers are set up as the same as the case study 1. But the maximum PV power is, now, 0 kW (night time). The simulation results are shown in Fig. 6. Load power of phase A is the highest (20 kW). The inverter currents of phase B and C are shifted 180°, as in Fig. 6(a), which indicate that the inverter absorbs energy from the grid by phase B and C, and then injects again to the grid by phase A. Fig. 6(b) illustrates that the inverter absorbs power from the grid approximately 3.5 kW (negative value) by phase B and C while injects power to the grid approximately 7 kW by phase A (positive value). Then the grid powers on three phases are 13.4 kW, 13.15 kW and 13.05 kW at phase A, B, and C, respectively. These powers approximate to the average power of load power (13.3 kW). This is one of the inherent differences between PV inverter with and without imbalance load compensation function. In this case study, the standard deviation of the grid power is 0.1472 instead of 4.714 as the standard deviation of the load power.

3.3 Case study 3: Transient conditions

A 10 kW power load is suddenly disconnected at 0.15 s on phase B. Now, the load powers are 20 kW, 0 kW, and 10 kW at phase A, B, and C, respectively. The inverter absorbs 10 kW power from the grid through phase B and then re-delivers them back to the grid by phase A, as in Fig. 7(a). The inverter output power on phase C is almost 0 kW. The imbalance load is compensated successfully for all three phases even when one phase is disconnected and during the transient period. The transient time of the inverter is approximately 60 ms (~4 cycles) and then recovers the steady-state.

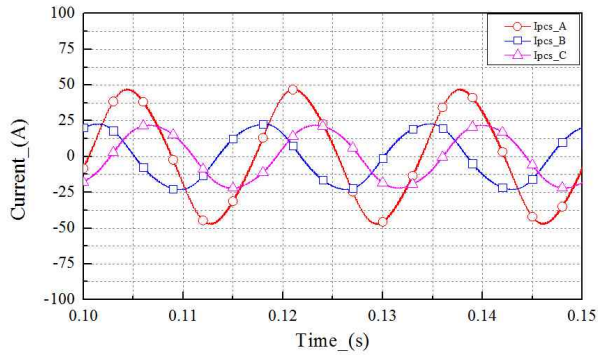

(a) The inverter output current waveforms

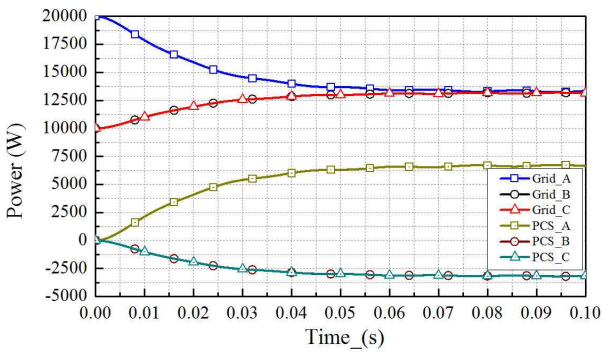

(b) The inverter output and grid power comparison

Fig. 6. Imbalance load compensation without PV power

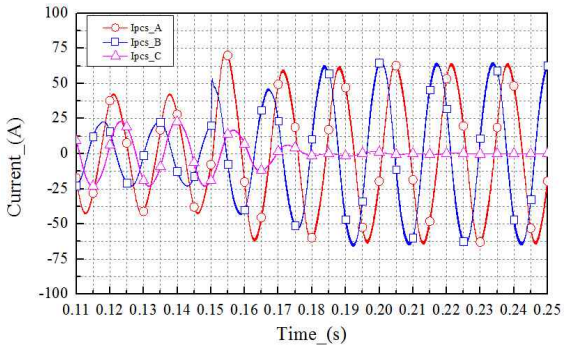

(a) The inverter output currents in transient period

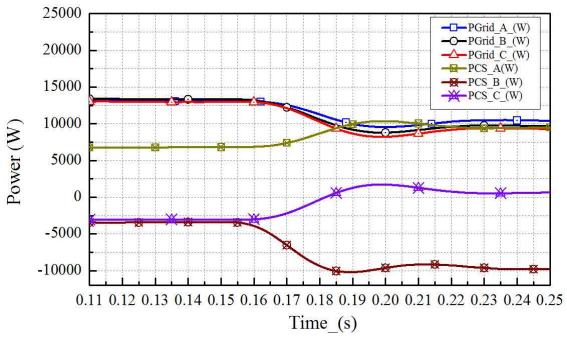

(b) The inverter output and grid power comparison in transient period

Fig. 7. Transient response of the PV inverter

Conventional PV inverter transfers only maximum PV power to the grid with balance power in the three phases. But the PV inverter with imbalance power load compensation function has different characteristics. When the maximum PV power is higher than the imbalance power, the PV power will be transferred to the grid with imbalance power in three phases which mean that the imbalance power is supplied by the inverter but not the grid. On the contrary, if the maximum PV power is smaller than the imbalance load power, the inverter will receive the power from the grid through one or two phase and then redistributes this power to the load via other phases. Consequently, the power supplied to the load of the grid is in balance between three phases.

4. Discussions

One of the most challenges of the PV inverter with imbalance load compensation function is controlling imbalance output currents of the PV inverter. The challenges of the PV inverter with imbalance load compensating function is simply overcome by the proposed control algorithm which transforms all time-varying reference signals to constant at two different rotating reference frames. Firstly, the proposed control algorithm has fully conventional function of a general PV inverter to transfer maximum PV power and control independently active and reactive power into the grid by a PI controller at the 60 Hz rotating reference fame. The imbalance load power is compensated by the PI controllers in the 120 Hz rotating reference frame. The maximum PV power was transferred to the grid and the imbalance power load was compensated successfully by the proposed control algorithm in both day-time, nigh-time, and during the transient period as depicted in Fig. 5, 6 and 7.

Dead-beat (DB), proportional-resonant (PR) and Fuzzy controllers were proposed to control a time-varying reference signal in power-active filter, motor control, and also inverter system and have impressive performance [1, 5-7, 13]. The advantages of the DB controller are accuracy, and fast response. The output signal can track the reference signal after several control cycles and can be predicted. However, it requires both precise model of the control object and delay of controller, measurement, and PWM generator. The PR controller was proposed to control a sinusoidal reference signal at a specific frequency [6, 7, 13]. The PR control has large high gain at only selected frequency but has no effect to other frequency signal. However, in practical, there are still many problems related to stability and implementation [13]. That's why it is not suitable for commercial products in mass production. The fuzzy logic and hysteresis controllers are suggested to control the inverter as in [12, 14-16]. The hysteresis has complicated switching state due to its non-linear characteristic. The fuzzy logic, otherwise, requires high mathematical skill to understand and implement it to the system.

The control algorithm is proposed to simply overcome the difficulties of controlling a time-varying signal a three-phase four-wire PV inverter with imbalance load compensation function. However, this is only able to apply to the inverter with imbalance load power compensation function. The proposed control algorithm should be more studied to apply to other applications.

5. Conclusion

In this paper, a new control algorithm has been proposed for a three-phase four-wire PV inverter with imbalance load compensation function. The control algorithm includes dc-link voltage controller and current controllers in two different rotating frames. It fully takes advantages of the conventional PI controller in a general inverter such as independent active-reactive power control, zero steady-state error, stability, and simplicity. The simulations of the PV inverter with imbalance power compensation function are carried out using PSIM in three difference cases. The simulation results demonstrate that the proposed control algorithm has good performance for imbalance power compensation. The standard deviation of grid power reduces significantly compared to one of the load power. The proposed control algorithm can be effectively utilized to a three-phase four-wire PV inverter with imbalance power compensation function.

Acknowledgements

This research was supported by Korea Electric Power Corporation [Grant number: R16XA01]

References

[1] N. Jenkins, R. Allan, P. Crossley, D. Kirschen and G. Strbac, *Embedded Generation,* IET, 2000, p.1-10.

[2] Nikos Hatziargyrion, Microgrids; *Architechtures and Control*, IEEE Press Wiley, 2014, pp. 1-35.

[3] Gyeong-Hun Kim, Chulsang Hwang, Jin-Hong Jeon, Jong-Bo Ahn and Eung-Sang Kim, "A Novel Three-phase Four-leg Inverter based Load Unbalance Compensator for Stand-alone Microgrid," *Electrical Power and Energy Systems*, vol. 65, pp. 70-75, 2015.

[4] Chang-Soon Kim, Chulsang Hwang, Gyeong-Hun Kim, Minwon Park, In-Keun Yu, "Three-phase four-leg type PCS with individual phase control algorithm for compensating unbalance loads using ESS," *in Proceeding of IEEE PEDS*, pp. 903-907, Jun. 2015.

[5] Haitham Abu-Rub, Mariusz Malinowski and Kamal Al-Haddad, *Power Electronics for Renewable Energy*

Systems, Transportation and Industrial Applications, IEEE WILEY, 2014, pp. 560-564.
[5] A. Sahara, A. Kessal, L. Rahmani and J. P. Gaubert, "Improved Sliding Mode Controller for Shunt Active Power Filter," *JEET,* vol. 11, no. 3, pp. 662-669, May, 2016.
[6] C. Lascu, L. Asiminoaei, I. Boldea, and F. Blaabjerg, "High Performane Current Controller for Selective Harmonic Current Compensation in Active Power Filter," *IEEE Trans. on Power Electronics*, vol. 22, no. 5, pp. 1826-1835, Sept. 2007.
[7] S. Buso, L. Malesani, and P. Mattavelli, "Comparison of Current Control Techniques for Active Filters Applications," *IEEE Trans. on Ind. Electron.*, vol. 15, no. 5, pp. 722-729, Oct. 1998.
[8] J. C. Basilio, and S. R. Matos, "Design of PI and PID controllers with transient performance specification", *IEEE Trans. on Education*, vol. 45, no. 4, pp. 364-370, Nov.2002.
[9] A. K. Al-Othman, M. Alsharidah, N. A. Ahmed and B. Alajmi "Model Predictive Control for Shunt Active Power Filter in Synchronous Reference Frame", *JEET.*, vol. 11, no. 1, pp. 709-718, Mar. 2014.
[10] Xie Bin, Dai Ke, and Kang Yong, "DC Voltage Control for thre Three-Phase Four-Wire Shunt Split-capacitor Active Power Filter," *in preceding of 9th Int. Electric Machines and Drives Conf*., vol. 15, no. 2, pp. 1669-1673, May 2009.
[11] F. Briz, M. W. Degner, and R. D. Lorentz, "Analysis and Design of Current Regulators using Complex Vectors," *IEEE Trans. on Ind. Appl*., vol. 36, no. 3, pp. 817-825, May/June. 2000.
[12] Chennai Salim, Benchouia M-T and Golea A., "Harmonic Current Compensation based on Three-phase Three-Level Shunt Active Filter using Fuzzy Logic Current Controller," *JEET*, vol. 6, no. 5, pp. 595-604, Sept. 2011.
[13] D.V. Le, S. M. Park, M. Park, and I. K. Yu, "Hardware-Based Implementation of a PIDR Controller for Single-Phase Power Factor Correction," *KSIIS*, vol. 21, no. 4, pp. 21-30, Aug. 2016.
[14] K. Basaran, and N. S. Cetin, "Designing of a fuzzy controller for grid connected photovoltaic system's converter and comparing with PI controller," *in Proceeding of IEEE ICRERA*, pp. 102-106, Nov. 2016.
[15] F. Ronilaya, J. Miyauchi, and A. Kurniawan, "PID-Type Fuzzy Controller for Grid-Supporting Inverter of Battery in Embedded Small Variable Speed Wind Turbine," *JPEE*, vol. 2, no. 5, pp. 151-160, Apri. 2014.
[16] M. Venkatesan, R. Rajeswari, and N. Deverajan, "A Fuzzy Logic Based Three phase Inverter with Single DC Source for Grid Connected PV System Employing Three Phase Transformer," *JEER*, vol. 5, no. 3, pp. 739-745, Jun. 2015.

Ding-Vuong Le received B.S. and M. S. degrees in Electrical Engineering from Hanoi University of Science and Technology, and Changwon National University, respectively. His research interests are electromagnetic launch technologies for cold-launching system, pulsed power system, power converter system, and renewable energy applications.

Chang-Soon Kim He received B.S and M.S degrees in electrical engineering from Changwon National University in 2014. His research interests are renewable energy sources, power conversion equipment and signal processing.

Byeong-Soo Go received B.S. and M.S. degrees in Electrical Engineering from Changwon National University in 2013 and 2015, respectively. His research interests are electromagnetic launch technologies for cold-launching system, pulsed power system, wind turbine, and superconducting applications devices.

Minwon Park He received B.S degree in Electrical Engineering from Changwon National University in 1997 and his M.S. and Ph.D. degrees in Electrical Engineering from Osaka University in 2000 and 2002, respectively. His research interests are the development of the simulation model of power conversion equipment and renewable energy sources using EMTP type Simulators.

In-Keun Yu He received B.S degree in Electrical Engineering from Dongguk University in 1981 and his M.S. and Ph.D. degrees in Electrical Engineering from Hanyang University in 1983 and 1986, respectively. His research interests are electric energy storage and control systems, PSCAD/EMTDC and RTDS simulation studies, and renewable energy sources.